University of Tehran

Earth Observation and Geomatics Engineering

Online ISSN: 2588-4360

Homepage: https://eoge.ut.ac.ir/

Damage detection using Gas Neural Network and Statistical Analysis using Very High-Resolution Imagery; Application to Beirut 2020 Explosion

Sara Khanbani [1], ***Reza Shah-Hosseini*** [2✉], *and* ***Saeid Homayouni*** [3]

1. School of Surveying and Geospatial Engineering, College of Engineering, University of Tehran, Tehran E-mail: sara.khanbani@ut.ac.ir

2. Corresponding author, School of Surveying and Geospatial Engineering, College of Engineering, University of Tehran, Tehran. E-mail: rshahosseini@ut.ac.ir

3. Centre Eau Terre Environnement, Institut national de la recherche scientifique (INRS), Quebec G1K 9A9, Canada. E-mail: saeid.homayouni@inrs.ca

Article Info

Article type:
Research Article

Article history:
Received 2024-06-25
Received in revised 2024-12-01
Accepted 2025-03-02
Available online 13 May 2025

Keywords:
Beirut explosion,
Change Detection,
Gas Neural Network (Gas-NN),
Damage Assessment,
Multi-resolution Segmentation (MRS).

ABSTRACT

Change detection (CD) in urban and natural areas using Very High-Resolution (VHR) satellite images is essential for damage assessment, urban expansion, and environmental analysis. Traditional supervised machine learning techniques face challenges due to urban environments' spatial and spectral complexity and the difficulty in obtaining extensive training data. This paper introduces an unsupervised CD method for MAXAR VHR images, which addresses these challenges by eliminating the need for prior knowledge. Our approach integrates Multi-Resolution Segmentation (MRS) and the Gas Neural Network (Gas-NN) algorithm to enhance feature extraction and selection. We extract textural and spectral features from pre- and post-event images, using correlation analysis to identify and retain features with high discriminant capability. The Interquartile Range (IQR) method identifies and removes outlier data, thereby improving data quality. The difference map generated from these features is segmented using MRS, with segments represented by their mean pixel values. These segments are then clustered using the Gas-NN algorithm, where the cluster with the highest center values is identified as the changed cluster. Our method achieves an overall accuracy of 97.68% based on ground truth data, demonstrating its effectiveness in automatic CD without extensive training data. This approach shows significant potential for applications in damage assessment, urban expansion, and environmental analysis, marking an advancement in Earth observation and remote sensing.

Cite this article: *Khanbani, S., Shah-Hosseini, R., & Homayouni, S. (2025). Damage Detection using Gas Neural Network and Statistical Analysis using Very High-Resolution Imagery; Application to Beirut 2020 Explosion. Earth Observation and Geomatics Engineering, Volume 8 (Issue 1), Pages 13-28. http//doi.org/10.22059/eoge.2025.378566.1154*

Publisher: University of Tehran.

DOI: http//doi.org/10.22059/eoge.2025.378566.1154

1. Introduction

Change Detection (CD) is a fundamental method used to discern changed and unchanged areas within images acquired from different sensors or the same sensor at different times, depicting the same geographical scene. The output of this process is a change map, which stands as a crucial product providing insights into the alterations observed. These alterations hold significant implications in various Earth surface monitoring applications, including forest degradation monitoring in the Amazon, agricultural expansion tracking in Southeast Asia, disaster assessment in earthquake-prone regions like Japan, and evaluation of environmental effects on ecosystems such as coral reefs (Chughtai, Abbasi, and Karas 2021; Shao et al. 2021; Sun et al. 2021; He et al. 2021) Several factors influence the CD process on Remote Sensing (RS) images, such as seasonal changes, atmospheric conditions, vegetation variations, and building shadows. Historically, CD techniques relied primarily on the spectral information of individual pixels. However, with technological advancements, state-of-the-art techniques have evolved to incorporate spatial, textural, and spectral information, enabling more accurate and comprehensive detection and mapping of changes. For instance, integrating high-resolution satellite imagery and machine learning algorithms has significantly improved the accuracy of deforestation detection in tropical rainforests (Shi et al. 2021). These advanced techniques have greatly enhanced the capabilities of CD in RS, allowing for a more in-depth analysis of the ever-changing Earth's surface. The development of remote sensing (RS) sensors in recent decades and the ability to acquire high-resolution RS images have provided a unique opportunity for researchers in various fields (Chughtai, Abbasi, and Karas 2021). These high spatial resolution satellite images facilitate urban feature extraction, such as buildings, roads, and trees, and allow for the efficient detection and mapping of their changes (Shao et al. 2021). For example, modern sensor like the WorldView-3 can capture images with a spatial resolution of up to 30 cm, enabling detailed analysis of urban infrastructure and landscape modifications. This advancement in RS technology has significantly complemented the CD process, enabling more precise analysis of alterations on Earth's surface, such as monitoring urban sprawl in rapidly growing cities and assessing damage from natural disasters with greater accuracy. Most CD methods are applied through two primary strategies: pixel-based and object-based methods (Chughtai, Abbasi, and Karas 2021). Pixel-based methods analyse individual pixels to detect changes, whereas object-based methods, like post-classification CD, focus on larger image segments or objects. Post-classification CD is an object-based method that compares land cover maps from two or more observation times. This technique classifies the pre- and post-event images separately to map the land covers and then compares the classification results to produce the final change map. However, since the classification accuracy directly affects the land cover information, any classification errors can significantly impact the resulting change map. For instance, misclassifying urban areas as vegetation in either the pre- or post-event image can lead to incorrect CD, highlighting the importance of accurate classification in the CD process. The pixel-based methods are based on a pixel-by-pixel comparison of two images acquired at two different times. The difference images highlight the changed areas of the scene and can also determine the nature of the change (Shao et al. 2021). The change map's accuracy primarily depends on the input images' geometric, spectral, and radiometric quality. Satellite observations are inevitably influenced by the atmosphere, necessitating the adoption of specific techniques to mitigate these effects. Among such techniques are image ratioing and spectral or textural differencing, which prove valuable in minimizing the impact of atmospheric distortions on the acquired data. Supervised and unsupervised CD methods have recently been developed (He et al. 2021; Shi et al. 2021; Sun et al. 2021). In most existing studies, both pre-event and post-event images (multi-temporal approaches) (Zhang et al. 2020; Lv et al. 2019) were generally used, and some of them also used post-event images (single post-event images) (Nie, Zeng, and Jiao 2019; Abdi, Esfandiari, and Jabari 2021).Multi-temporal approaches require pre-processing steps, including registration and correcting radiometric and atmospheric effects for pre- and post-images (Zhang et al. 2020; Lv et al. 2019). Supervised methods combine expert knowledge and the ability to access ground truth data for algorithm training. When the type of change is needed, supervised methods are preferred. Post-classification comparison is a supervised CD method that classifies images independently and then compares the classified results. In this manner, the operation of such methods is complicated in practical scenarios. A timely and accurate change map is essential for disaster management and assessment, especially for emergency response. Automatic or semi-automatic techniques for extracting change information are widely required. Collecting ground truth data for the training phase of the supervised technique is time-consuming. Although supervised methods can produce better results in some cases than unsupervised methods, they

have high priority in practice because of no dependency on ground truth data, so they attracted extensive attention from researchers (Shao et al. 2016). Recent advances in remote sensing have expanded change detection methods beyond traditional pixel-based and object-based approaches. Emerging techniques now integrate geometric, spectral, and temporal data for enhanced urban analysis. Three-dimensional methods, utilizing LiDAR and photogrammetry, address limitations of 2D approaches by incorporating elevation data. Machine learning further enhances these techniques, enabling automated and scalable solutions for complex urban environments (Hosseini, Seyedeh Sharareh, and Tabib Mahmoudi Fatemeh, 2021). This study addresses the challenge of change detection following the Beirut explosion using a novel unsupervised approach based on segmentation and texture features. By using pre- and post-event very high-resolution images, the method employs feature selection, multi-resolution segmentation, and clustering via a Gas Neural Network to identify significant changes. The proposed framework ensures robust and insightful analysis, effectively capturing impacted areas and advancing object-based change detection methodologies.

2. The Related Work

Several studies have focused on unsupervised CD methods (Fang, Du, and Wang 2022; Zou et al. 2022). Most related studies use the unsupervised CD method based on difference images and change vector analysis (Zou et al. 2022). For a low or medium-spatial resolution of a satellite image in which a pixel represents a large geographic area and may involve several terrestrial objects, neighboring pixels can be assumed independent, and pixel-based comparisons can be practical and efficient. Nevertheless, the pixel independence assumption in VHR Images with a high spatial resolution is false, so it is necessary to model pixel adjacency and consider their spatial-textural information (Shafique et al. 2022). Sudipansaha et al. presented unsupervised CD context-sensitive framework-deep change vector analysis for CD in multi-temporal VHR images. The Convolutional neural network features are exploited. To have an unsupervised system, the spatial relationship between neighboring pixels and the complex object starts from a suboptimal pre-trained multilayered CNN for obtaining deep features (Saha, Bovolo, and Bruzzone 2019). Tobias proposed the object-based approach for an unsupervised CD focused on individual buildings. The principal component analysis (PCA) is a unique procedure for determining relevant principal components. K-means clustering is applied to discriminate between changed and unchanged buildings. Several groups of object-based difference features derived from multi-temporal VHR data are evaluated regarding their discriminative properties for CD. In addition, the influence of deviating from viewing geometries when using VHR data acquired by different sensors is quantified (Leichtle et al. 2017) . Kun Tan proposed an object-based approach for an automatic CD using multiple classifiers and multi-scale uncertainty analysis in high-resolution images. The Gray-level co-occurrence matrix (GLCM), morphological, and Gabor filter texture features are extracted to construct the input data and spectral features. In addition, a random forest is used to select the features and determine the optimal feature vectors forCD. Change vector analysis (CVA) based on uncertainty analysis is then implemented to choose the initial training samples. According to the diversity, support vector machine (SVM), k-nearest neighbor (KNN), and extra-trees (ExT) classifiers are then chosen as the base classifiers for Dempster-Shafer (D-S) evidence theory fusion, and unlabelled samples are selected using an active learning method with spatial information. Finally, multi-scale object-based D-S evidence theory fusion and uncertainty analysis are used to classify the difference image (Tan et al. 2019). Kevin et al. proposed an unsupervised CD method using a convolutional neural network. In this research, the convolutional neural network method is implemented for the semantic segmentation of the input image. The feature map is generated at different levels from before and after images. Then, the difference image is generated at each level using the absolute difference operator. The final change map is generated at each level using the optimum threshold value and the energy function that makes the relationship between input images. Sicang et al. proposed an unsupervised band expansion method to produce spectral and spatial bands to enhance the distinction of the changing area of multispectral images. In particular, the proposed method uses two simple nonlinear multiplications, and Division has been used to develop spectral bands. The multidimensional morphology reconstruction method has been used to develop the spatial information of the bands. Three unsupervised methods have also been used to evaluate the proposed method (Liu et al. 2019) .The deep neural network-based CD methods require extensive training data databases to train the neural network accurately - examining and determining the number of neural network layers and filters. There are many predefined criteria for convolutional neural networks, so choosing the right network for each piece of data is vital. Adjusting learning weights between different layers of the neural network is very challenging. On the other hand, high-resolution images contain much information about land features. The complexity of spatial characteristics of urban landscapes requires complex processing. Therefore,

proposing an approach capable of accommodating the intricacies of high-resolution images while minimizing complexity holds significant promise in this context.

3. The Proposed Method

To solve the CD problem caused by the Beirut explosion using high-resolution images - a strategy for detecting unsupervised changes based on segmentation has been presented. The conceptual model of the method is illustrated in Figure 1. The proposed unsupervised (CD) analysis for very high-resolution (VHR) images leverages texture features from the Maxar project, primarily focusing on object-based analysis. This approach significantly enhances the informativeness of the images, leading to more robust and insightful results.

First, texture features are extracted from both pre-event and post-event images. A selection process is employed based on the correlation coefficient between the extracted features to identify the most relevant features. An absolute difference image is then computed using these optimal features. To ensure the reliability of the difference image, Range Analysis is performed, effectively eliminating any outliers or irregularities in the data. Additionally, the absolute difference image derived from the spectral bands of the images undergoes segmentation using the multi-resolution segmentation method. This method partitions the image into meaningful regions. An image entropy analysis is conducted to determine the most suitable segmentation results, identifying segments that encapsulate valuable information.

In the subsequent phase, the average value of each segment's absolute difference features image is designated as a segment indicator. These segment indicators serve as essential characteristics for further analysis. The Gas Neural Network method is then applied to cluster these segments based on their respective indicators, grouping them into coherent categories. The resulting clusters are scrutinized based on their cluster centers. Among these clusters, the highest cluster center values are identified as the "changed segments." This process effectively pinpoints the areas in the image where significant changes have occurred, providing valuable insights for CD analysis.

3.1. Texture extraction

Texture as a spatial feature model is the spatial relationship between the Gray levels of image pixels. It significantly impacts pattern recognition with various textures in the image. Usually, these differences cannot be recognized only by using the main spectral values of images.

Various methods have been developed to produce spatial features (texture). These techniques are divided into four general categories: statistical, geometric, model base, and signal processing (filtering). Gray Level Co-occurrence Matrix (GLCM) is one of the most efficient techniques for texture extraction using remote sensing images. GLCM was introduced in 1973 by Haralick (Löfstedt et al. 2019; Haralick, Shanmugam, and Dinstein 1973). This matrix consists of $G \times G$ cells, each equal to $pd, d = (d_x + d_y)$ and the displacement vector. $Pd\,(i,j)$ also equals the number of repetitions of the gradient pairs i and j spaced d apart. Table 1 represents the Texture descriptors proposed by Haralick.

3.2. Feature Selection Strategy Incorporating Correlation Coefficient and p-Value Evaluation

The generation of efficient feature space in the CD is challenging. In this way, the efficient feature space is defined as a space in which the unrelated problem-solving features are removed, with no data redundancy. Feature selection is one of the major steps in the pre-processing of many machine-learning applications (Xue et al. 2021) .

The method of dimension reduction of the feature selects appropriate features from the main feature space according to an evaluation function. It also reduces the feature data that has created redundancy in the entire feature set. Feature selection means selecting features that provide the most differentiation and separation (Xue et al. 2021)Thus, selecting different subsets of features and examining them based on different criteria is necessary to create a suitable feature set. One of the feature selection criteria is the degree of data dependency, which can be called the correlation between data (Zhou, Wang, and Zhu 2022).Pearson correlation (equation 1) is used to find the relationship between continuous features. Correlation is one of the famous measurements of similarity between two features. If two features are linearly related, their correlation coefficient is +1 and -1. Their correlation coefficient is zero if the features are independent (Hsu and Hsieh 2010).

$$\rho_{X,Y} = \frac{cov(X,Y)}{\sigma_X \sigma_Y} = \frac{E[(X-\mu_X)(Y-\mu_Y)]}{\sigma_X \sigma_Y} \quad (1)$$

Analyze the correlation matrix to identify features with correlation coefficients close to +1 or -1, indicating strong correlation. Retain one feature from each correlated pair to reduce redundancy, as highly correlated features provide similar information. Features with coefficients around 0 suggest low or no correlation and may be valuable for retaining unique information.

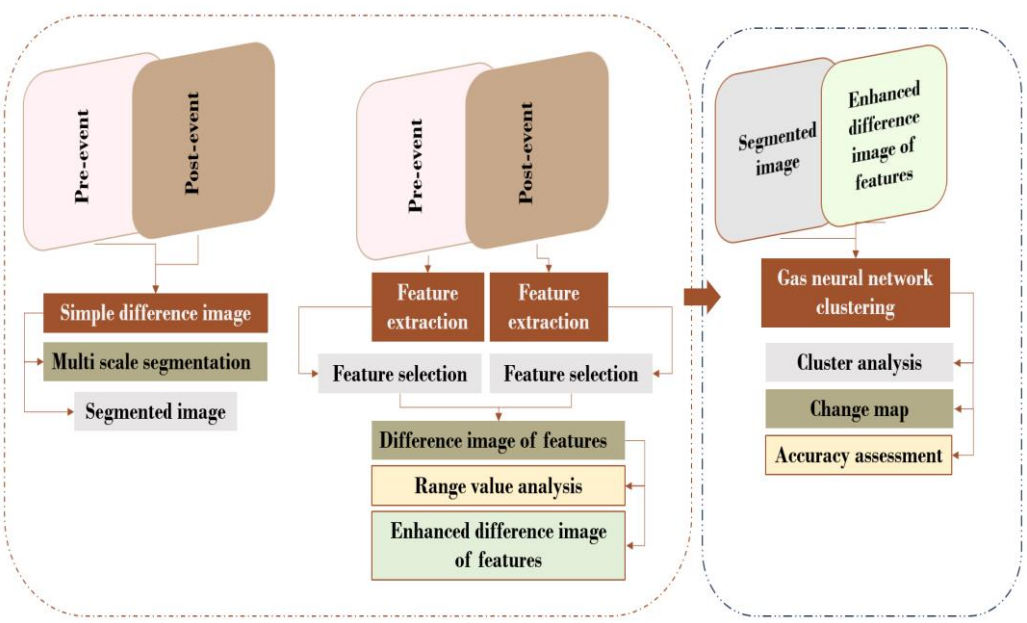

Figure 1. The conceptual procedure of the proposed method

Table 1: Texture descriptors proposed by Haralick (Felipe, Traina, and Traina 2003)

Descriptor	***Equation***	***Meaning***
Variance	$\sum_i \sum_j (i-j)^2 P(i,j)$	*Level of image contrast*
Entropy	$\sum_i \sum_j (i-j)^2 \, log \, P(i,j)$	*Suavity of image*
Energy	$\sum_i \sum_j P^2(i,j)$	*Uniformity of image*
Homogeneity	$\sum_i \sum_j P(i,j)/(1+\lvert i-j \rvert)$	*Homogeneity of pixels' distribution*
Moment	$\sum_i \sum_j (i-j)^3 P(i,j)$	*Level of distortion*
Inverse variance	$\sum_i \sum_j P(i,j)\,/(i-j)^2$	*Inverse level of contrast*

Using the correlation coefficient as a criterion for dimensionality reduction is well-supported in the literature. Chormunge and Jena (2017) proposed a method that integrates clustering with correlation measures to produce an effective feature subset, demonstrating that the elimination of irrelevant features via clustering followed by the selection of non-redundant features using correlation measures significantly enhances the efficiency and accuracy of the feature selection process. Their experimental results, evaluated on Microarray and Text datasets, revealed the superiority of this approach over other renowned feature selection methods using a Naïve Bayes classifier (Chormunge and Jena 2018). By employing the correlation coefficient, we aim to identify and retain the most informative features that contribute to the CD process while eliminating those that introduce redundancy. This approach not only simplifies the model but also improves its generalizability and performance for each texture feature, perform a hypothesis test to compute the corresponding p-value, indicating the probability of observing the data under the null hypothesis. Set a significance threshold (commonly $\alpha = 0.05$*) to evaluate the p-values. A low p-value (*$p \leq 0.05$*) provides strong evidence against the null hypothesis, suggesting the texture feature is significantly related to the target variable and should be selected. Conversely, a high p-value (*$p > 0.05$*) indicates weak evidence, implying that the texture feature may be irrelevant and can be discarded.*

3.3. Range Value Analysis

*Range Value Analysis is a statistical technique commonly used for dataset outlier detection. This method examines the distribution of data points and identifies outliers based on quartile ranges and the interquartile range (IQR). The procedure involves several steps including the calculation of the first quartile (Q1) and third quartile (Q3) to determine the IQR, defined as IQR = Q3 - Q1. It sets lower and upper boundaries at Q1 - 1.5 * IQR and Q3 + 1.5 * IQR, respectively, and any data points outside these boundaries are flagged as outliers. Figure 2 shows the steps of Range Value Analysis (Seo 2006).*

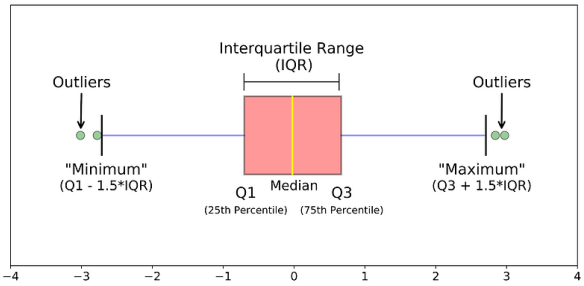

Figure 2. Range Value Analysis Procedure

3.4. Absolute Difference Image

Suppose two images $X_1 = \{x_1(i,j) | 1 \leq i \leq M, 1 \leq j \leq N\}$, $X_2 = \{x_2(i,j) | 1 \leq i \leq M, 1 \leq j \leq N\}$

$$DI(i,j) = |x_1(i,j) - x_2(i,j)| \quad (2)$$

M × N dimensions obtained from the same geographical areas and at two different times have been studied. The simple difference (DI) image is calculated from the difference between the values of the features in the first and second-time images according to equation 2 (Khanbani, Mohammadzadeh, and Janalipour 2020).

3.5. Multi-scale segmentation

Multi-scale segmentation refers to the technique of merging pixels or visual objects at different scales. This process often utilizes a bottom-up classification algorithm based on a two-by-two region merging technique. In this approach, the algorithm classifies visual objects into three categories:1. Seed: The initial point of reference for merging. 2. Candidate: Potential objects that may merge with the seed. 3. Target: The result of the merging process (Ming et al. 2015). The segmentation process follows a structured sequence to ensure accuracy and efficiency. It involves several key stages: Identifying Potential Pairs: The first step is to find the best pair of pixels or regions for potential merging based on their similarity Designating a New Seed: In the second stage, the best candidate that has been identified becomes the new seed, while objects that do not meet the criteria for a two-sided best fit are excluded from consideration. Merging Image Objects: In the third stage, the algorithm merges image objects when a two-sided best fit between the seed and candidate is established, combining them into a single region. Iterative Processing: The fourth step involves checking each image object uniquely during each loop of the merging process. This loop continues until no further mergers can be made or a stopping condition is met. Comparison and Adjustment: Lastly, the potential outcomes of all merger candidates are compared in detail against the seed and candidate structures to determine the best possible merging strategy (Liu, Du, and Mao 2017). the segmentation process relies on establishing local homogeneity, which is assessed through two main factors: Spectral Homogeneity: This considers the similarity in pixel color or intensity. Structural Homogeneity: This assesses the spatial arrangement and shape of the regions. The combination of these two types of homogeneity helps refine the segmentation and ensures that merged regions truly represent coherent features in the image (Liu, Du, and Mao 2017). The segmentation consists of five main stages. The first step is to look for the best pair for potential integration with the best fit. In the second step, the best candidate image object becomes the new seed without the best two-sided fit, and the best fit is searched. The image objects are merged in

the third step when the best fit is two-sided. In the fourth step, in each loop, each image object is controlled once on the object, and the loops continue for as long as possible (Kurtz et al. 2010; Duan, Zhang, and Zhang 2020).

3.6. Entropy test

Entropy is a statistical measure often used to quantify the amount of uncertainty or disorder in a system. In the context of image analysis, it helps assess the level of randomness or complexity in the pixel values of a given region. Heterogeneous regions of the image have a high degree of irregularity. Homogeneous regions have a small amount. According to this definition, the entropy parameter can be used to analyze segmentation results If a segment is homogeneous, low entropy value founded since the distribution of pixel values will be concentrated around a few values. Heterogeneous Regions: Conversely, a heterogeneous segment will yield a higher entropy value due to the multitude of pixel values contributing to a more complex distribution. Segmentation Quality Assessment: By evaluating the entropy of segmented regions:High entropy in a segmented region might indicate that the segmentation has not effectively identified distinct features and that the segment is too broad or includes too much variation. Low entropy might indicate a successful segmentation, where distinct homogeneous according to the equation 3(Xu, Shin, and Klette 2014).

3.7. Segments Feature

This step uses the difference image output based on the pixel step 3.2, and the segmentation output is applied to the difference image in step 3.4. It is necessary to extract the corresponding features of each segment. The average statistics of the feature corresponding to each segment will be calculated.

3.8. Gas Neural Network

The gas neural network method is an artificial neural network designed to determine the optimal data representation based on the available feature vectors without assuming an initial network topology(Sledge and Keller 2008) . Neurons within the Gas neural network dynamically adapt to feature vectors and exhibit behaviours akin to Gases diffusing within feature space. This adaptability has proven highly valuable in applications such as vector or content quantification, data compression in image processing and voice recognition, and pattern recognition. In a Gas neural network, during each iteration and for each input data point V in space M, the distortion set defined for the existing network with n nodes is as follows (equation 4).

$$D_v = \{\|v - w_i\| \ , \quad i = 1, \dots, n\} \qquad (4)$$

In this relation w_i is the weight assigned to each node. When new data are entered, a sequence of elements v set D_v help to update the weights. The neural network upgrade results in "the winner take the most" instead of referring to the "winner take all" rule. In the Gas neural network, neurons try to adapt to a similarity measure to input data. One of the similarity criteria is distance. By defining parameters such as rank k_i and learning decline , the adjustment stage for w_i is defined by the following relation. For each neuron, a rank of 0 to $n-1$ is defined for each data. Rank means the number of better neurons for each neuron than the selected neurons for the studied data. Suppose we are examining the second neuron; we can determine how many neurons are in a better position than one data set compared to the second neuron.

$$w_i^{new} = w_i^{old} + \epsilon e^{-k_i/\lambda}(v - w_i^{old}) \qquad (5)$$

λ specifies the number of nerve nodes whose weight varies significantly. If parameter λ tends to zero, it becomes WTA: the winner takes all, and if it tends to infinity, it becomes constant and uniform learning by all units. In the form of gas-neural learning, we will have something in between(Fritzke 1994). ϵ or step size is a number to indicate the maximum amount of consistency in the update steps. If, for data, one neuron wins the first rank and the other neuron wins the second rank, it indicates a logical relationship between neurons. The first and second ranks are defined based on the concept of graph edges. For each update, a time is established. If the connection between the edges is not strengthened after a certain duration, the edge will be removed. If the connection between the first and second-rank neurons is still maintained during each update, the associated edge will be strengthened, and its age will increase. The steps are repeated until the stop condition is reached and the location of the optimal neurons is determined (Sledge and Keller 2008; Fritzke 1994; Palomo and López-Rubio 2016). Figure 3 shows the gas neural network process. Figure 3 shows Gas neural network process

3.9. Accuracy assessment

Manually selected test data were used to evaluate and analyse each step. Change, non-change, and overall accuracy parameters have been used for accuracy and precision assessment. The change and un-change accuracy mean the percentage of changed and unchanged pixels correctly identified in the created change map. The overall accuracy is the percentage of the sum of the changed and unchanged pixels that have been correctly identified in the change map. ***4. Experiments***

4.1. Study area

The selected study area for this research is in the port area of Beirut, Lebanon, located in the southwest on the shores of the Mediterranean coast. Beirut is a city scarred by a turbulent civil war and home to approximately 2 million

residents. The local time zone follows UTC + 2 (Eastern European Time, EET); during summer, it shifts to UTC + 3 (Eastern European Summer Time, EEST). On August 4, 2020, at approximately 18:08 local time (15:08 UTC), a catastrophic explosion rocked the Lebanese port area of Beirut. The explosion, equivalent to an earthquake with a local magnitude (ML) of 3.3 according to the US Geological Survey (USGS), resulted in the tragic loss of over 100 lives and inflicted severe damage on nearby buildings. The aftermath of the explosion left at least 300,000 people homeless, with estimated damages ranging between 10 and 15 billion US dollars. Figure 4 shows the top view of Beirut Explosion on geographical map.

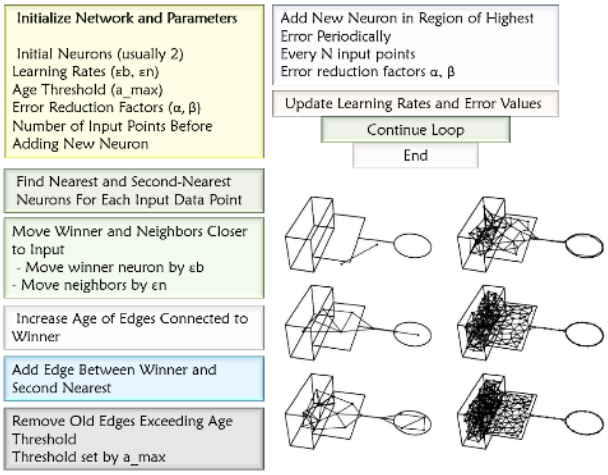

Figure 3. Schematic representation of topology identification using a gaseous neural network (Sledge and Keller 2008; Fritzke 1994).

4.2. Dataset Description

The dataset used in this study comprises high-resolution satellite images obtained through the MAXAR / globe project. MAXAR Technologies provided Worldview-2 satellite products, which offer the following characteristics:

***Spatial Resolution:** Worldview-2 images have a spatial resolution of 0.46 meters in the panchromatic band and 1.84 meters in the multispectral bands. This high spatial resolution allows for detailed analysis of urban areas and infrastructure.*

***Spectral Bands:** The satellite captures imagery in 8 **multispectral** bands (providing valuable spectral information for various remote sensing applications.*

***Coverage:** Worldview-2 provides extensive coverage over urban and rural areas, offering a comprehensive view suitable for monitoring natural disasters and urban development. Maxar's Worldview-2 satellite products covered a significant portion of Beirut, facilitating detailed analysis before and after the tragic explosion on August 4, 2020.*

4.3. Results

The database introduced in Sections 4.2 was used to evaluate the proposed algorithm's performance. Then the corresponding Haralick features were extracted from the images before and after the event, and features with high information content were extracted using correlation analysis. The difference image corresponding to the features with high content is calculated. After identifying the outlier values by the black box statistical method and removing the outlier values, and scaling the data, a difference image using the black box statistical method, removing the outlier values, and scaling the data, a difference image from the enhanced features is created. The absolute difference image of spectral values is also segmented using multi-resolution analysis, and the appropriate segmentation result is selected based on the entropy.

In the next step, the corresponding feature for each segment is calculated based on the average image values of the difference between improved features. The calculated features for each segment are entered into the gas neural network, and the segments are clustered unsupervised. The final binary change map is obtained by analyzing the values of the cluster's center.

In Figure 5, high-resolution red-green-blue (RGB) MAXAR images are displayed over the study area. Figure 5(a) represents the area after the explosion, while Figure 5(b) depicts the area before the event occurred. Subsequently, the following step involves the creation of an absolute difference image based on the spectral values. Figure 5(c) illustrates the resulting absolute difference image derived from the spectral.

Figure 4: Top view of Beirut explosion on map

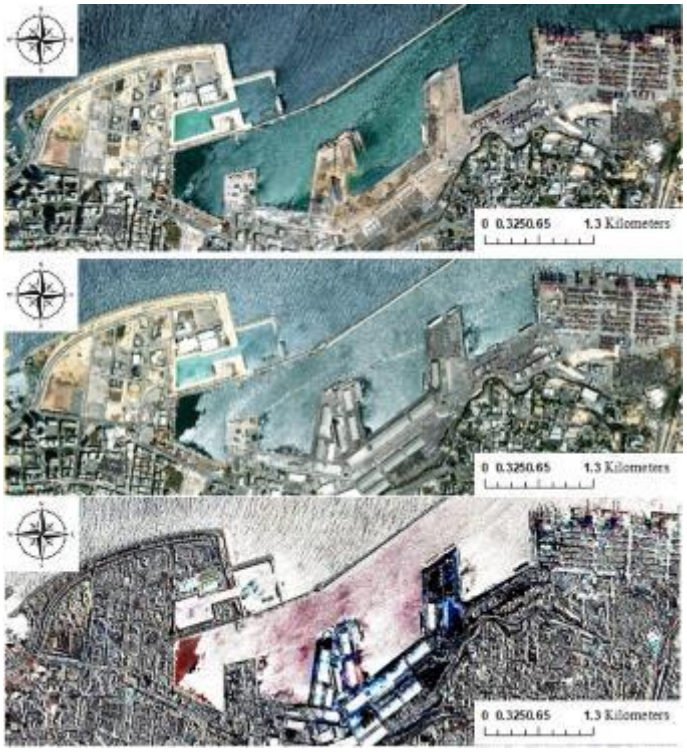

(a)

(b)

(c)

Figure 5: Beirut explosion (a) post-event and (b) pre-event. (c) absolute difference image of spectral values.

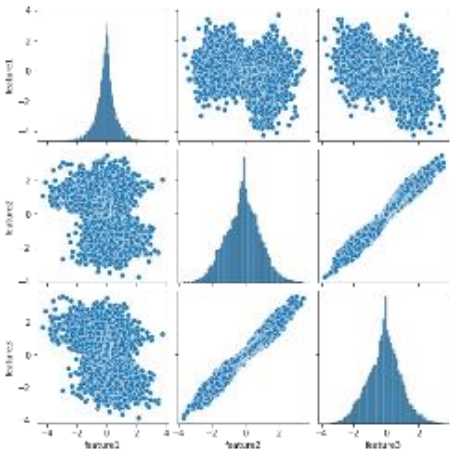

Figure 6: an example of correlation analysis for three texture features

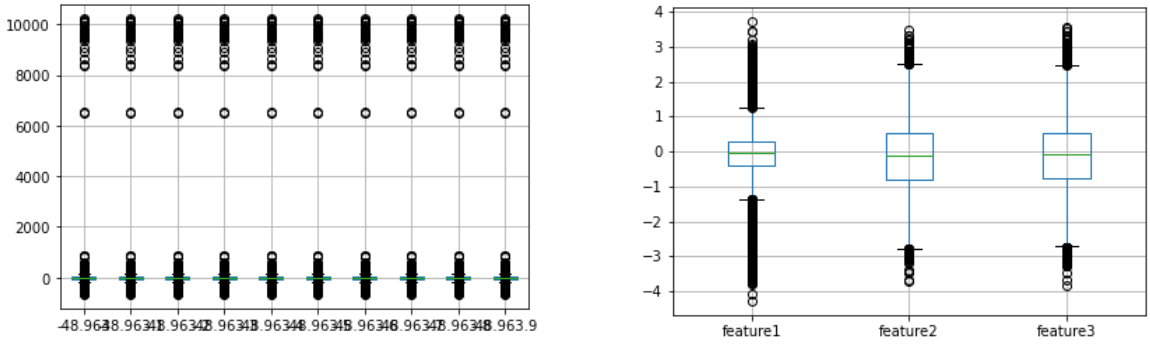

(a) *(b)*

Figure 7: (a) Schematic representation of Range Analysis before removing outlier data corresponding to all Haralick features. (b) Schematic representation of box plot test for three features with high information content after removing outlier data.

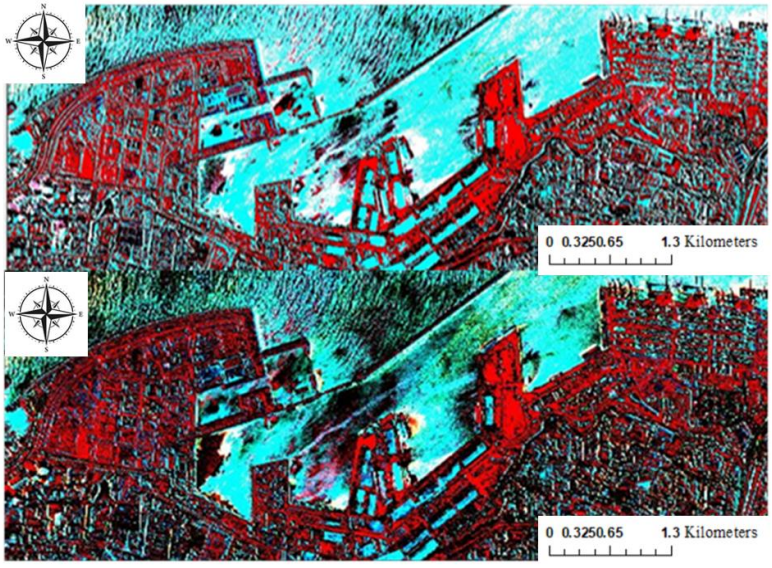

(a)

(b)

Figure 8: (a)absolute difference image calculated of effective texture features. (b) an improved absolute difference image of effective texture features.

Table2: The values of the input parameters of the gas neural network (Sledge and Keller 2008; Fritzke 1994).

Parameter	*Value*	*Justification*
N	*5*	*Number of neurons in the neural network. This value is chosen to balance computational complexity and network effectiveness.*
Max it	*50*	*Maximum number of iterations for network training. Higher iterations allow for a more thorough convergence of the network.*
T max	*100*	*Maximum number of iterations for adjusting network parameters. This parameter ensures sufficient time for network adaptation.*
ϵ initial	*2*	*Initial learning rate. Higher initial rates facilitate faster convergence during the early stages of training.*
ϵ final	*0.5*	*Final learning rate. Decreasing the learning rate over iterations stabilizes training and improves network generalization.*
λ initial	*2*	*Initial neighborhood radius. A larger initial radius helps capture a broader range of input data during the initial stages of training.*
λ final	*2*	*Final neighborhood radius. Maintaining a constant neighborhood radius stabilizes network performance during later iterations.*
T initial	*0.05*	*Initial temperature parameter. This parameter controls the magnitude of network updates during the initial training stages.*
T final	*0.5*	*Final temperature parameter. Increasing the temperature parameter towards the end of training helps fine-tune network parameters.*

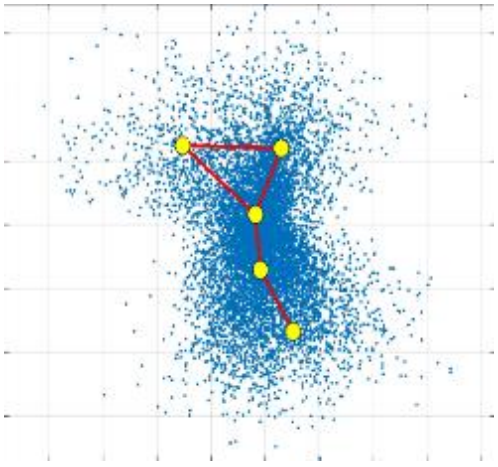

Figure 9: Schematic representation of the gas neural network operation in the spectral features of study area

The Haralick feature images were extracted from both input images. Furthermore, the optimal features were selected using correlation analysis, favouring features with low correlation values. An example of this correlation analysis for three features is depicted in Figure 6. As depicted in Figure 6, it is evident that the third and first features, as well as the second and first features, exhibit a low correlation, while the second and third features display

a high correlation. Consequently, in the context of change detection within this study area, it is reasonable to consider that the third and first features, or alternatively, the second and first features, may prove to be valuable. The subsequent step involves generating the absolute difference image an image different from these selected effective features. In Figure 8(a), the image depicts the absolute difference derived from the relevant features of the input images. Following the creation of this absolute difference image, it becomes imperative to eliminate any noise and outlier values, thereby ensuring that the difference image is scaled appropriately. The black box test calibrates the values t . To identify and address these outliers, the black box test is employed to calibrate the values. In Figure 7(a) and Figures 7(a) and 7(b), there is a schematic representation illustrating the statistical analysis of the black box both before and after the removal of outlier data, respectively. Following removing outlier data and scaling image values, an enhanced difference image is generated, as presented in Figure 8(b). The subsequent step involves calculating the mean values of the pixels within the improved difference image corresponding to each segment. These mean values are designated as segment indicators. Subsequently, these segment indicators serve as inputs for the Gas neural network clustering process, where a network with five nodes is utilized. The result of this clustering process yields the clustered image. Figure 9 provides a two-dimensional representation of the Gas neural network operation within the study area. In this figure, the yellow dots symbolize the network nodes, while the red lines represent the edges that facilitate maximum adaptability within the network. Table 2 shows the values of the input parameters of the Gas neural network. The clustered image of the output of the Gas neural network output in five clusters is shown in Figure 10(a). The reason for choosing five clusters was the different levels of changes in the image, including vehicles and sea wave differences. After producing the clustered image, the cluster centre with the highest centre value is considered a changed segment, and other clusters are considered unchanged. Figure 10(c) shows the output of the binary change map. Table 2 shows the values of input parameters of Gas Neural network that commonly used.

To assess the effectiveness of the proposed method, a total of 243,331 pixels representing definite and intended changes within the region were carefully chosen, alongside 919,540 pixels representing regions without definitive changes. When analysing the output change map, it became evident that the method achieved 100% accuracy in identifying the changing areas. Furthermore, the proposed method demonstrated its capacity to identify all desired changes within the area of interest correctly.

Concerning the "no-change" class, an impressive accuracy of 97.06% was achieved. This slightly lower accuracy was attributed to actual regional changes, such as alterations in roadways and bodies of water, which were not the primary focus of the analysis but were nonetheless detected by the method. In summary, the proposed method achieved an impressive overall accuracy of 97.68% compared to the ground truth image, affirming its robustness and reliability in detecting changes within the studied area.

In Figure 10(b), we can observe the ground truth accuracy image, meticulously crafted by an expert. Clustering, as an exploratory data analysis technique, aims to uncover inherent structural groups within the data. While it does not assign category labels, clustering has demonstrated its effectiveness in unsupervised CD within remote sensing applications. One of the enduring and widely utilized algorithms for clustering, even after nearly 50 years since its inception, is the k-means algorithm. This method remains a cornerstone in clustering, especially in remote sensing applications. For comparative assessment, Haralick features are computed from pre- and post-event images, and these features are employed to create a binary change map. This approach allows for evaluating and comparing different change detection methods and their performance against the ground truth data. Simultaneously, meaningful insights for CD are extracted through cluster centre analysis. Figures 10(d) and 10(e) display the binary change maps resulting from applying K-Means clustering to the datasets. According to the results, K-Means clustering achieves accuracy rates of 97.06%, 60.01%, and 89.28% for the unchanged, changed, and overall accuracy, respectively. These results indicate that the proposed method presented in this paper outperforms K-Means clustering when applied to very high-resolution (VHR) data in an unsupervised manner. The proposed method demonstrates its effectiveness in accurately detecting changes within the dataset, surpassing the performance of the traditional K-Means clustering approach.

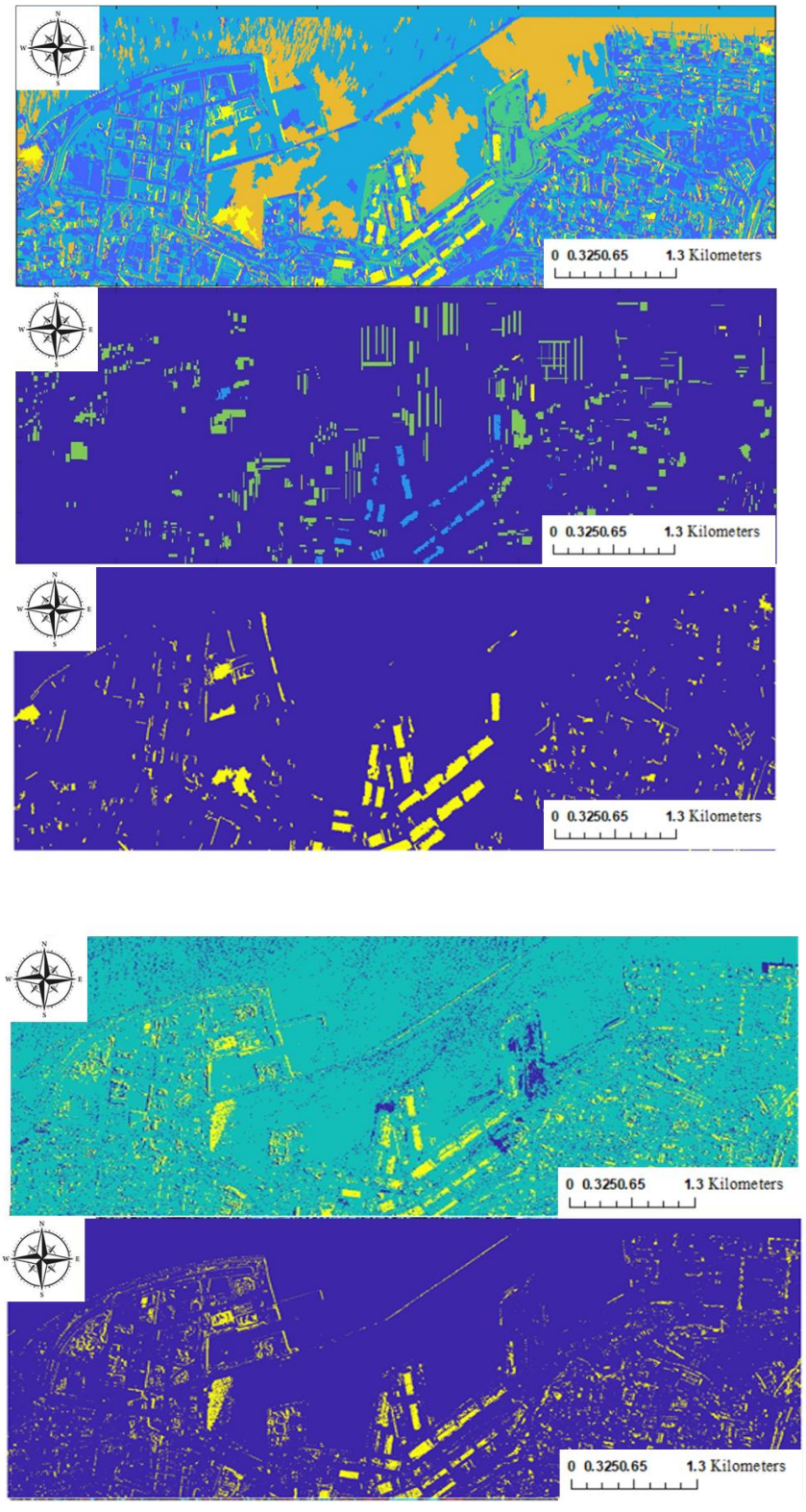

(a)

(b)

(c)

(d)

(e)

Figure 10: (a) clustered image from the Gas neural network, (b) ground truth image, (c) binary change map of the proposed method, (d) clustered image from the K-Means, (e) binary change map of K-Means

5. Conclusion

In this study, we presented an unsupervised CD methodology using high-resolution images, specifically focusing on detecting changes caused by the Beirut explosion. Change detection is a fundamental method utilized to distinguish altered and unaltered areas within images acquired at different times, and it holds significant implications for various Earth surface monitoring applications. The output of the CD process, the change map, provides valuable insights into observed alterations, aiding in disaster investigation, environmental monitoring, and more.

We proposed a multi-step approach based on segmentation and texture analysis to address the complexities of CD in high-resolution imagery. The proposed method involves extracting texture features from pre- and post-event images, then selecting features based on correlation coefficients and p-values to create an efficient feature space. An absolute difference image was then calculated to highlight the changed areas of the scene, while multi-scale segmentation was employed to divide the image into different segments based on spatial distribution. The entropy test was utilized to select appropriate segmentation results, enhancing the method's accuracy. Our methodology also incorporated the Gas neural network, a dynamic and adaptable artificial neural network, to obtain optimal data representations without predefined topology. By employing these advanced techniques, we achieved accurate and unsupervised CD, providing a timely and reliable change map essential for disaster management and emergency response scenarios.

In conclusion, our unsupervised CD methodology utilizing texture analysis and segmentation presents a valuable contribution to remote sensing and Earth observation. With its ability to accurately and automatically detect changes in high-resolution images, this approach holds promise for supporting disaster management, urban planning, and environmental monitoring efforts, providing valuable insights into the ever-changing Earth's surface. As technology advances, we anticipate further improvements in CD methods, enhancing our understanding of dynamic changes occurring in our environment.

Acknowledgment

We would like to thank MAXAR for providing the image dataset used in this research. The availability of this valuable dataset has been instrumental in our study and has significantly contributed to the outcomes of this paper.

References

Abdi, Ghasem, Morteza Esfandiari, and Shabnam Jabari. 2021. "Building damage detection in post-event high-resolution imagery using deep transfer learning." In 2021 IEEE International Geoscience and Remote Sensing Symposium IGARSS, 531-34. IEEE.Doi: 10.1109/IGARSS47720.2021.9553720.

Chormunge, Smita, and Sudarson Jena. 2018. 'Correlation based feature selection with clustering for high dimensional data', Journal of Electrical Systems and Information Technology, 5: 542-49. https://doi.org/10.1016/j.jesit.2017.06.004

Chughtai, Ali Hassan, Habibullah Abbasi, and Ismail Rakip Karas. 2021. 'A review on change detection method and accuracy assessment for land use land cover', Remote Sensing Applications: Society and Environment, 22: 100482. https://doi.org/10.1016/j.rsase.2021.100482

Duan, GongHao, JunChi Zhang, and Shuiping Zhang. 2020. 'Assessment of landslide susceptibility based on multiresolution image segmentation and geological factor ratings', International journal of environmental research and public health, 17: 7863. https://doi.org/10.3390/ijerph17217863

Fang, Hong, Peijun Du, and Xin Wang. 2022. 'A novel unsupervised binary change detection method for VHR optical remote sensing imagery over urban areas', International Journal of Applied Earth Observation and Geoinformation, 108: 102749. https://doi.org/10.1016/j.jag.2022.102749

Felipe, Joaquim Cezar, Agma JM Traina, and Caetano Traina. 2003. "Retrieval by content of medical images using texture for tissue identification." In 16th IEEE Symposium Computer-Based Medical Systems, 2003. Proceedings., 175-80. IEEE. DOI: 10.1109/CBMS.2003.1212785

Fritzke, B. 1994. 'A growing neural gas network learns topology', Advances in Neural Information Processing Systems, 7.

Haralick, Robert M, Karthikeyan Shanmugam, and Its' Hak Dinstein. 1973. 'Textural features for image classification', IEEE Transactions on systems, man, and cybernetics: 610-21.

He, Pengfei, Xiangwei Zhao, Yuli Shi, and Liping Cai. 2021. 'Unsupervised change detection from remotely sensed images based on multi-scale visual saliency coarse-to-fine fusion', Remote Sensing, 13: 630. DOI: 10.3390/rs13040630

Hsu, Hui-Huang, and Cheng-Wei Hsieh. 2010. 'Feature Selection via Correlation Coefficient Clustering', J. Softw., 5: 1371-77. DOI:10.4304/jsw.5.12.1371-1377

Khanbani, Sara, Ali Mohammadzadeh, and Milad Janalipour. 2020. 'Unsupervised change detection of remotely sensed images from rural areas based on using the hybrid of improved Thresholding techniques and particle swarm optimization', Earth

Science Informatics, 13: 681-94. https://doi.org/10.1007/s12145-020-00455-8

Kurtz, Camille, Nicolas Passat, Pierre Gançarski, and Anne Puissant. 2010. 'Multi-resolution region-based clustering for urban analysis', International Journal of Remote Sensing, 31: 5941-73. https://doi.org/10.1080/01431161.2010.512312

Leichtle, Tobias, Christian Geiß, Michael Wurm, Tobia Lakes, and Hannes Taubenböck. 2017. 'Unsupervised change detection in VHR remote sensing imagery–an object-based clustering approach in a dynamic urban environment', International Journal of Applied Earth Observation and Geoinformation, 54: 15-27. DOI: 10.1016/j.jag.2016.08.010

Liu, Jianhua, Mingyi Du, and Zhengyuan Mao. 2017. 'Scale computation on high spatial resolution remotely sensed imagery multi-scale segmentation', International Journal of Remote Sensing, 38: 5186-214. DOI: 10.1080/01431161.2017.1325536

Liu, Sicong, Qian Du, Xiaohua Tong, Alim Samat, and Lorenzo Bruzzone. 2019. 'Unsupervised change detection in multispectral remote sensing images via spectral-spatial band expansion', IEEE Journal of Selected Topics in Applied Earth Observations and Remote Sensing, 12: 3578-87. DOI: 10.1109/JSTARS.2019.2929514

Löfstedt, Tommy, Patrik Brynolfsson, Thomas Asklund, Tufve Nyholm, and Anders Garpebring. 2019. 'Gray-level invariant Haralick texture features', PloS one, 14: e0212110. https://doi.org/10.1371/journal.pone.0212110

Lv, Zhiyong, Tongfei Liu, Cheng Shi, Jon Atli Benediktsson, and Hejuan Du. 2019. 'Novel land cover change detection method based on K-means clustering and adaptive majority voting using bitemporal remote sensing images', Ieee Access, 7: 34425-37. DOI: 10.1109/ACCESS.2019.2892648

Ming, Dongping, Jonathan Li, Junyi Wang, and Min Zhang. 2015. 'Scale parameter selection by spatial statistics for GeOBIA: Using mean-shift based multi-scale segmentation as an example', ISPRS Journal of Photogrammetry and Remote Sensing, https://doi.org/10.1016/j.isprsjprs.2015.04.010

Nie, Yuliang, Qiming Zeng, and Jian Jiao. 2019. "Building Damage Assessment from Post-Event Polsar Image Based on Opce and Template Matching." In IGARSS 2019-2019 IEEE International Geoscience and Remote Sensing Symposium, 9402-05. IEEE. DOI: 10.1109/IGARSS.2019.8898951

Palomo, Esteban J, and Ezequiel López-Rubio. 2016. 'The growing hierarchical neural gas self-organizing neural network', IEEE transactions on neural networks and learning systems, 28: 2000-09. DOI: 10.1109/TNNLS.2016.2570124

Saha, Sudipan, Francesca Bovolo, and Lorenzo Bruzzone. 2019. 'Unsupervised deep change vector analysis for multiple-change detection in VHR images', IEEE transactions on geoscience and remote sensing, 57: 3677-93. DOI: 10.1109/TGRS.2018.2886643

Seo, Songwon. 2006. 'A review and comparison of methods for detecting outliers in univariate data sets', University of Pittsburgh.

Shafique, A, G Cao, Z Khan, M Asad, and M Aslam. 2022. "Deep Learning-Based Change Detection in Remote Sensing Images: A Review. Remote Sens. https://doi.org/10.3390/rs14040871

Shao, Pan, Wenzhong Shi, Pengfei He, Ming Hao, and Xiaokang Zhang. 2016. 'Novel approach to unsupervised change detection based on a robust semi-supervised FCM clustering algorithm', Remote Sensing, 8: 264. DOI: 10.3390/rs8030264

Shao, Pan, Wenzhong Shi, Zhewei Liu, and Ting Dong. 2021. 'Unsupervised change detection using fuzzy topology-based majority voting', Remote Sensing, 13: 3171. https://doi.org/10.3390/rs13163171

Shi, Qian, Mengxi Liu, Shengchen Li, Xiaoping Liu, Fei Wang, and Liangpei Zhang. 2021. 'A deeply supervised attention metric-based network and an open aerial image dataset for remote sensing change detection', IEEE transactions on geoscience and remote sensing, 60: 1-16. DOI: 10.1109/TGRS.2021.3085870

Sledge, Isaac J, and James M Keller. 2008. "Growing neural gas for temporal clustering." In 2008 19th International Conference on Pattern Recognition, 1-4. IEEE. DOI: 10.1109/ICPR.2008.4761768

Sun, Yuli, Lin Lei, Dongdong Guan, and Gangyao Kuang. 2021. 'Iterative robust graph for unsupervised change detection of heterogeneous remote sensing images', IEEE Transactions on Image Processing, 30: 6277-91. DOI: 10.1109/TIP.2021.3093766

Tan, Kun, Yusha Zhang, Xue Wang, and Yu Chen. 2019. 'Object-based change detection using multiple classifiers and multi-scale uncertainty analysis', Remote Sensing, 11: 359. DOI: 10.3390/rs11030359

Xu, Zezhong, Bok-Suk Shin, and Reinhard Klette. 2014. 'Accurate and robust line segment extraction using minimum entropy with Hough transform', IEEE Transactions on Image Processing, 24: 813-22. DOI: 10.1109/TIP.2014.2387020

Xue, Yu, Haokai Zhu, Jiayu Liang, and Adam Słowik. 2021. 'Adaptive crossover operator based multi-objective binary genetic algorithm for feature selection in classification', Knowledge-Based Systems, 227: 107218. DOI: 10.1109/TIP.2014.2387020

Zhang, Chenxiao, Peng Yue, Deodato Tapete, Liangcun Jiang, Boyi Shangguan, Li Huang, and Guangchao Liu. 2020. 'A deeply supervised image fusion network for change detection in high resolution bi-temporal remote sensing images', ISPRS Journal of Photogrammetry and Remote Sensing, 166: 183-

200. https://doi.org/10.1016/j.isprsjprs.2020.06.003

Zhou, Hongfang, Xiqian Wang, and Rourou Zhu. 2022. 'Feature selection based on mutual information with correlation coefficient', Applied Intelligence, 52: 5457-74. https://doi.org/10.1007/s10489-021-02524-x

Zou, Lidong, Muyi Li, Sen Cao, Feng Yue, Xiufang Zhu, Yizhan Li, and Zaichun Zhu. 2022. 'Object-oriented unsupervised change detection based on neighborhood correlation images and k-means clustering for the multispectral and high spatial resolution images', Canadian Journal of Remote Sensing, 48: 441-51. https://doi.org/10.1080/07038992.2022.2056434

Hosseini, Seyedeh Sharareh, and Tabib Mahmoudi Fatemeh, 2021. "Review on 2D and 3D Building Change Detection Methods Based on Remotely Sensed Data." JOURNAL OF ENVIRONMENTAL SCIENCE AND TECHNOLOGY, 23(7110001640), PP. 191-206. DOI: 10.30495/jest.2022.50484.4976

Kevin et al (2019). Unsupervised Change Detection in Satellite Images Using Convolutional Neural Networks. In 2019 International Joint Conference onNeuralNetworks(IJCNN).IEEE.https://doi.org/10.1109/IJCNN.2019.8851762